Novelty Journals

ISSN 2394-7349

International Journal of Novel Research in Engineering and Science
Vol. 11, Issue 1, pp: (55-71), Month: March 2024 - August 2024, Available at: www.noveltyjournals.com

Mechanical Behaviour, Wear Characteristics, and Biological Properties of Chitosan Particles-Keratinous Human Hair Fibre Reinforced High Density Polyethylene Matrix Hybrid Composite

Adewuyi BO[1], Daramola OO[1*], Adewole TA[1], Adediran AA[2,5*], Oyetunji A[1], Adefegha AS[3], Olasunkanmi OG[4]

[1]Department of Metallurgical and Materials Engineering, Federal University of Technology Akure, Nigeria

[2]Department of Mechanical Engineering, Landmark University, Omu-Aran, Kwara State

[3]Department of Biochemistry, Federal University of Technology Akure, Nigeria

[4]Department of Chemistry, Federal University of Technology Akure, Nigeria

[5]Department of Mechanical Engineering, University of Johannesburg, South Africa

DOI: https://doi.org/10.5281/zenodo.11161314

Published Date: 09-May-2024

Abstract: **High-Density Polyethylene (HDPE) matrix composites were developed using a compression moulding technique. Chitosan particles were chemically produced from deep-sea crab shells through deproteinization, demineralization, and 60% deacetylation methods. Human hair was treated with 5% NaOH and shredded into strands for use as reinforcement. Composites with varying weight fractions of chitosan particles (2, 2.5, 3, 3.5, and 4%) and human hair fibre (1, 2, 3, 4, and 5%) were developed at a moulding temperature of 180°C, under an applied pressure of 0.2 kPa. The composites showed improved mechanical properties. The best tensile strength (28.43 MPa) and tensile modulus (400.36 MPa) were achieved with 2.5 wt. % chitosan and 2 wt.% human hair fibre (Sample C). The highest hardness (51.52 HS) was found in Sample D with 3 wt.% chitosan and 3 wt.% human hair fibre. Impact strength consistently increased, with Sample D exhibiting the highest value (32.67 KJ/m^2). Wear resistance was best in Sample D. Scanning electron microscopic analysis revealed uniform reinforcement dispersion in Samples B, C and D, while voids were observed in Samples E and F. The voids acted as stress concentrators, causing material fracture. Antimicrobial tests indicated initial microbiological presence, which was eliminated after sterilization. The control sample showed the highest bacterial growth, while Sample F (4% chitosan + 5% HF) has the lowest capacity to sustain bacterial growth. This indicates that sample F is the best for biomedical applications since it has a total average colony count of 122 CFU/ml, which is lower than all other samples.**

Keywords: **High Density Polyethylene, Chitosan particles, Human hair fibre, Compression moulding technique, Deproteinization, and Antimicrobial.**

1. INTRODUCTION

Researchers have started conducting comprehensive studies into the biomedical exploitations of a few rarely requested biological wastes. This is in response to environmentalists concerns about ecological welfare and the skyrocketing demand for dependable and affordable biomaterials (Daramola *et al*., 2019; Kumar *et al*., 2015). Bird feathers and eggshells, mollusk shells, crab exoskeletons, fish scales, mammalian hair, horns, and hooves are typical examples of these wastes that are produced annually in billions of tonnes by agro-biological businesses (Daramola *et al*., 2019). The effective synthesis of vital biomaterials including keratin, chitosan, collagen, and hydroxyapatite from these wastes has been demonstrated by an

impressive number of study findings (Jayathilakan *et al*., 2012; Daramola *et al*., 2021). According to Jayathilakan *et al*. (2012), these synthetic biomaterials have desirable qualities such low weight, great biocompatibility, biodegradability, self-healing behavior, drug delivery, and the ability to heal wounds more quickly. These synthetic biomaterials have notable uses in regenerative medicine, biomaterials engineering, and minimally invasive surgery (Balaji *et al*., 2012; Croisier and Jérôme, 2013; Lee *et al*., 2013). Fair mechanical strength, moderate wear resistance, and high affinity for moisture uptake are some of the associated drawbacks that severely restrict their use in orthopedics and other fields where high strength, high wear resistance, and low moisture uptake are essential (Tran and Mututuvari, 2016). The cuticle, cortex, and medulla are the fundamental structural components of human hair. Outermost layer of the hair is referred to as the cuticle, and the cortex, which makes up the majority of the remaining region, is in the center. The deepest layer of human hair, the medulla, is the thinnest cylindrical component (Nanda and Satapathy, 2017). 45.68% carbon, 27.9% oxygen, 6.6% hydrogen, 15.72% nitrogen, and 5.03% sulfur make up the majority of the chemical elements in hair. According to Choudhry and Pandey, (2012), approximately 91% of the protein content in hair consists of long-chain amino acids, including cytosine, serine, glutamine, threonine, glycine, leucine, valine, and arginine. Notably, the linkage between cysteine molecules and keratin proteins forms robust disulfide chemical bonds, renowned for their exceptional strength which provide human hair its durability and resistance to breakdown under environmental stress (Hiwarkar *et al*., 2017). The excellent tensile strength, slow rate of degradation, hydrophilic characteristics, cost-effectiveness, special chemical structure, and elastic recovery attributes of human hair fibre constitute some of its qualities that makes it an attractive reinforcement material (Butt *et al*., 2016; Jain and Kothari, 2012; Vengatesan *et al*., 2017; Nanda and Satapathy, 2017; Hiwarkar *et al*., 2017). Studying the mechanical behavior of a polypropylene matrix and human hair fiber, Choudhry and Pandey, (2012) discovered that a composite containing 3-5 weight percent human hair fiber outperforms the neat polymer in terms of flexural strength, flexural modulus, and Izod impact strength; however, at 10-15 weight percent, it falls short of the unreinforced polymer in terms of flexural strength, flexural modulus, and impact strength. In similar research done by Babu *et al*. (2021), optimum results were obtained using a composite including hair measuring 20 mm in length and a concentration of 5 phr. Human hair significantly raised the sample's tensile strength by 44%, tear strength by 60%, hardness by 140%, and improved the abrasion resistance index by 44% after being added to the 5 phr sample.

As stated by Zhao *et al*. (2017), the biocompatibility, biodegradability, hydrophilicity, and antibacterial properties exhibited by chitosan render it a favorable choice for applications within the medical field. Because of its large molecular weight, high viscosity, and poor electrospinnability due to its restricted solubility, this polymer exhibits poor mechanical characteristics (Fukunishi *et al*., 2016). To limit its rapid degradation, enhance electrospinnability, and boost flexibility and elongation, chitosan is frequently mixed with other polymers, such as PCL, HDPE (Zirak *et al*., 2017). For tissue engineering purposes, synthetic polymers like polyethylene (PE), polycaprolactone (PCL), polyglycolic acid (PGA), polylactic acid (PLA), and polyether ether ketone (PEEK) hold promise due to their favorable biocompatibility and mechanical attributes (Puppi *et al*., 2010). Paxton *et al*. (2019) emphasized that high-density polyethylene (HDPE) stands as a remarkably versatile biomaterial, having demonstrated intriguing outcomes in pre-clinical investigations and clinical applications. Affordability, straightforward processing, and exceptional ductility are a few characteristics that encourage the usage of HDPE and allow for the insertion of a wide range of particle types in the polymer (Wang, 2003). Thus, even when loaded with a large number of fillers, innovative composites may be manufactured using the most widely used and least expensive melt extrusion processes (Wang, 2003; Lam and Wu, 2012). Shape memory polymers and polymers mixed with these waste-based biomaterials are quickly taking the place of the conventional metallic alloys used in biomedical applications (Bao *et al*., 2016). According to Jayathilakan *et al*. (2012) and Saini *et al*. (2015), these materials have a wide acceptance in the biomedical area because of their favorable features that outweigh those of metallic alloys. Although titanium alloys, nickel-titanium shape memory alloys, and stainless steel have all been widely used as implants over the past few decades, their high densities, high cost, and subsequent biomedical corrosion have forced a rethink (Scholz *et al*., 2011). The aforementioned alloys are eventually changed to prevent hazardous chemicals from being deposited into the host due to biomedical corrosion (Manivasagam *et al*., 2010). Their replacements typically need further surgery, which has a substantial expense attached with them (Schmutz *et al*., 2008). However, a thorough investigation in this field is deemed beneficial since the production of biocompatible polymer-based chitosan particles and treated human hair fibre composite for biomedical use is feasible. The major goal of this research is to develop high-density polyethylene matrix hybrid composites for biomedical applications that are reinforced with chitosan derived from crab shells and human hair fibres.

Chitosan will offer biocompatibility, anti-microbial and biodegradability to HDPE while human hair will improve the mechanical properties of HDPE.

Novelty Journals

ISSN 2394-7349

International Journal of Novel Research in Engineering and Science
Vol. 11, Issue 1, pp: (55-71), Month: March 2024 - August 2024, Available at: www.noveltyjournals.com

2. MATERIALS AND METHOD

MATERIALS

The materials employed in this study were as follows: Crab shells, human hair, High Density Polyethylene (HDPE 3408) having a density of 0.935-0.955 g/cm3, melt flow index of 3.5 to 6.5 g/10 min, a melt index ratio (MIR) of 10-30, NaOH (Assay of ≥ 90%, Sulphate of 0.002%, Phosphate of 0.001%, Iron of 0.001% and heavy metals of 0.002%), distilled water and Hydrochloric Acid (Specific gravity of 1.155, Sulphate of 3 ppm, Iron of 1ppm, free chlorine and bromine is 2ppm, heavy metals of 2ppm and sulphites of 3ppm). The Crab shells were sourced locally from a food restaurant in Lagos, Nigeria, human hair was gathered, treated and used as the fibre, High Density Polyethylene (HDPE) was procured in Lagos, Nigeria, HCL and NaOH were gotten from Pascal Scientific Akure, Nigeria.

SYNTHESIS OF CHITOSAN

Warm water was used to wash the crab shell's exoskeleton multiple times in order to get rid of soluble organics, adhesion protein, and other contaminants. After that, the shells were smashed with a mortar and pestle. To assist the chemical extraction of chitosan and to improve the quality of the chitosan, the crushed shells were stored in a polyethylene bag for 24 hrs at 25°C for partial autolysis. The three steps in chitosan extraction were deproteinization, demineralization, and deacetylation. Deproteinization was carried out by preparing a 3.5% NaOH solution which was diluted in a 1:10 (w/v) ratio with the shell powder. It was subsequently heated for two hrs at 65°C while being agitated in a water shaker bath. After that, it was separated by decantation and cleaned with aqua dest. It was constantly washed until the pH was neutral, then it was filtered using filter paper. After 24 hrs of drying at 90°C, it was weighed (Fatnah *et al*., 2019). Thereafter, demineralization process was done which involves mixing deproteinized crab shell powder with 1 N HCl solution at a ratio of 1:15 (w/v) for 30 minutes at room temperature. It was then separated by decantation and cleaned with aqua dest. It was constantly washed until the pH was neutral, then it was filtered. It was then dried for 24 hrs at 90°C in the oven. The chitin was then measured and weighed (Fatnah *et al*., 2019). Chitin from the results of mineral removal underwent deacetylation by being mixed with 50% sodium hydroxide (NaOH) solution with a ratio 1:10 (w/v), heated to 90°C in a water shaker bath while being swirled for two hrs, and then washed with aqua dest. Decantation was then used to separate it. After filtering, washing was continued until the pH was neutral. It was then dried for 24 hrs at 90°C in an oven before being weighed. The chitosan was then kept in a desiccator (Fatnah *et al*., 2019; Rahmi *et al*., 2017). Figure 1 shows the synthesis procedure.

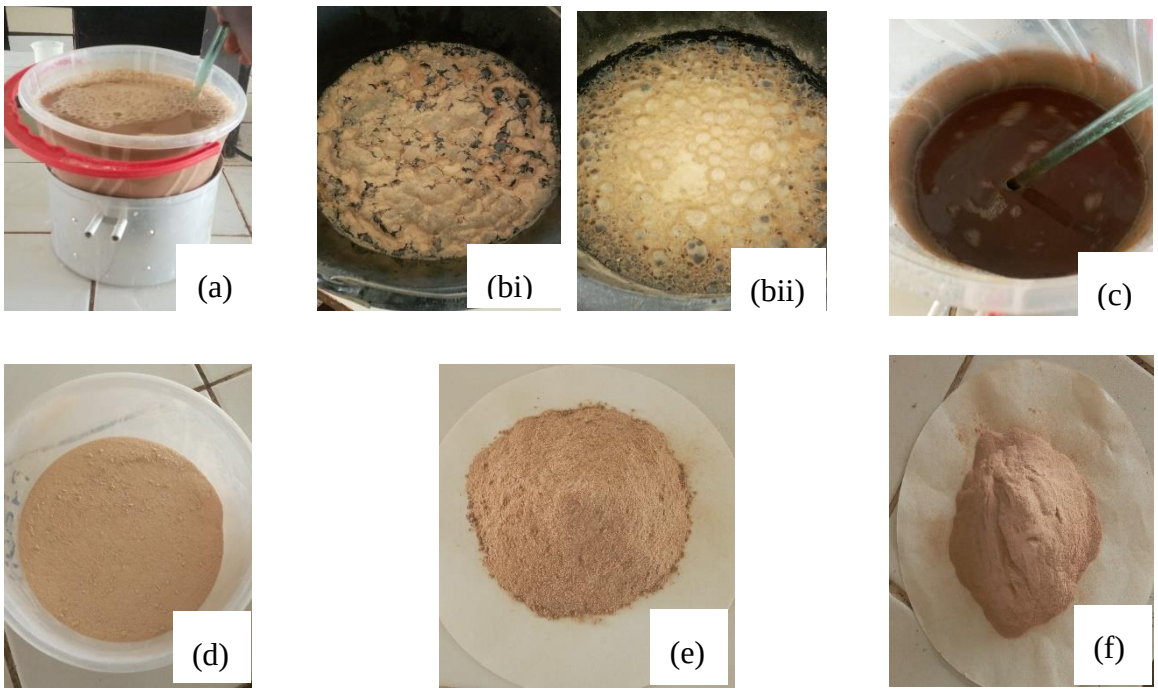

Figure 1: Extraction process of Chitosan from Crab shell (a) Deproteinization process (bi), (bii) Demineralization processes (c) Deacetylation process (d) Deproteinized sample (e) Demineralized sample (f) Deacetylated sample

ALKALI TREATMENT OF HAIR FIBRE

Waste human hair fibre was treated chemically and then utilized directly as a natural fibre. Hair was first cleaned in hot water to get rid of any oil or other impurities before being rinsed in pure ethanol to get rid of any organic materials that stuck to the hair fibre. The alcohol residues were removed from this hair fibre sample by washing it many times in distilled water (Prashant and Shishir, 2016). For 48 hrs, these fibres were dried in an oven to eliminate the water. A 5% NaOH solution was then made, and the dried hair fibre sample was placed within for 1 hour. After that, it was removed and repeatedly rinsed with distilled water to bring the alkali pH to a neutral state. Finally, the treated hair fibre sample was dried in the oven for another 48hrs. The purpose of treating hair with Sodium Hydroxide (NaOH) is to change the chemical structure of the hair so as to improve interfacial adhesion between the hair and polymer matrix which will improve the mechanical properties of the developed composite. Figure 2 shows the treatment process.

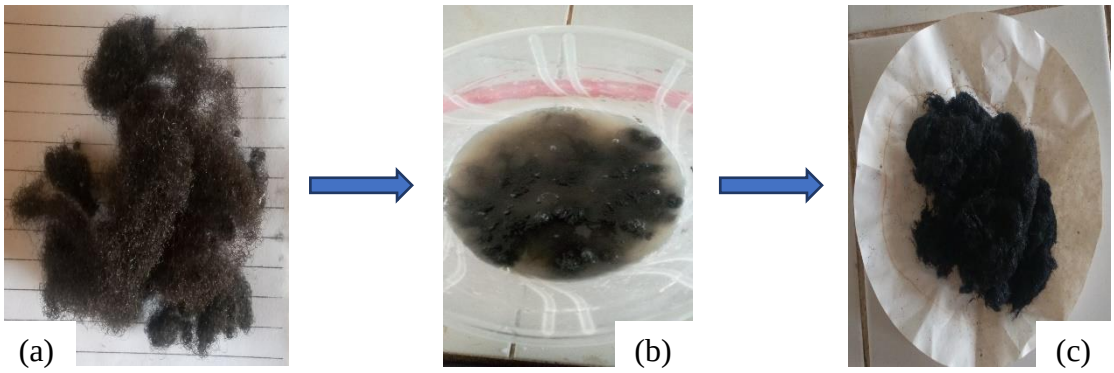

Figure 2: (a) Untreated HF sample (b) Treatment process (c) Treated HF sample

NB: HF is Hair Fibre

FOURIER TRANSFORM INFRA-RED SPECTROSCOPY

The chitosan particles were examined using Fourier transformed infrared (FTIR) spectroscopy, and a transmittance spectrum was produced. The sample's spectra were twice characterized using a Perkin Elmer Spectrum 100 spectrometer. The 550 to 4000 cm^{-1} wavelength range was chosen. To get a suitable signal-to-noise ratio, 32 spectra were co-added and averaged. The resolution of the spectra was always kept at 4 cm^{-1} and a gauge of 130.

XRD ANALYSIS OF THE SYNTHESIZED CHITOSAN PARTICLES

With the help of a wide-angle x-ray diffraction spectrometer (WAXD, Pan Analytical Xpert Pro Diffractometer, The Netherlands), the X-ray diffraction pattern of the synthesized chitosan particles was determined using a CuKa radiation with a wavelength of 0.154 nm, at a voltage of 45 kV, step size of 0.02º and a current of 40 mA.

COMPOSITIONAL ANALYSIS TEST

To perform the compositional analysis, 1–5g of oven-dried sample was weighed into a crucible, which was then put in a muffle furnace and heated to 450–550°C for 8–12 hrs. 10 ml of 6 M HCl was used to wash any ash from the crucible into the beaker after the ash had been transferred to a 100 ml Pyrex beaker. The beaker was put on a hot plate with a watch glass covering it, and it was heated to a controlled boil. When the acid level in the beaker is almost at its lowest point, the mixture is taken off the hot plate and filtered using ashless filter paper (Whatman No. 41). Distilled deionized water should be used to rehydrate the volume to 50 or 100 ml.

SCANNING ELECTRON MICROSCOPY

Using an AURIGA Scanning Electron Microscopy (SEM) with an accelerating voltage of 15 kV, the surface morphology of the produced composite samples was investigated. Prior to being analyzed using a scanning electron microscope (SEM), the compression-moulded samples were first cryogenically fractured in liquid nitrogen. The cryo-fractured and notched impact fractured surfaces were mounted on aluminum stubs and sputter coated with gold using an EMITECH K950X sputter coater.

Novelty Journals

ISSN 2394-7349

International Journal of Novel Research in Engineering and Science
Vol. 11, Issue 1, pp: (55-71), Month: March 2024 - August 2024, Available at: www.noveltyjournals.com

COMPOSITE FORMULATION

Table 1 displays the formulation table for the HDPE-based composites

Table 1: Hybrid composites formulation

S/N	Designation	HDPE (wt.%)	Chitosan (wt.%)	HF (wt.%)
1	A (control)	100	0	0
2	B	97	2	1
3	C	95.5	2.5	2
4	D	94	3	3
5	E	92.5	3.5	4
6	F	91	4	5

NB: HDPE: High Density Polyethylene

HF: Hair fibre

PRODUCTION OF HDPE/CHITOSAN-HF COMPOSITES

Human hair fibers, chitosan, and HDPE were combined using a twin-screw extrusion technique. Measured HDPE is melted by the Twin-extruder (Leistritz ZSE 27 MAXX), which also equally distributes measured chitosan and human hair fibers throughout the polymer matrix. The molten material is then pushed through a die to cool and solidify into an extrudates. The extrudates were grinded in a grinding machine. The grinded extrudates were then moulded into different test specimens of HDPE matrix composite using Carver hydraulic Laboratory Press (3852-004) at a moulding temperature of 180 °C and under a pressure of 5 MPa. When the created samples had cooled to room temperature, the test specimens were then taken out of the mould. The procedure was repeated to produce unreinforced HDPE, which was utilized as a control sample.

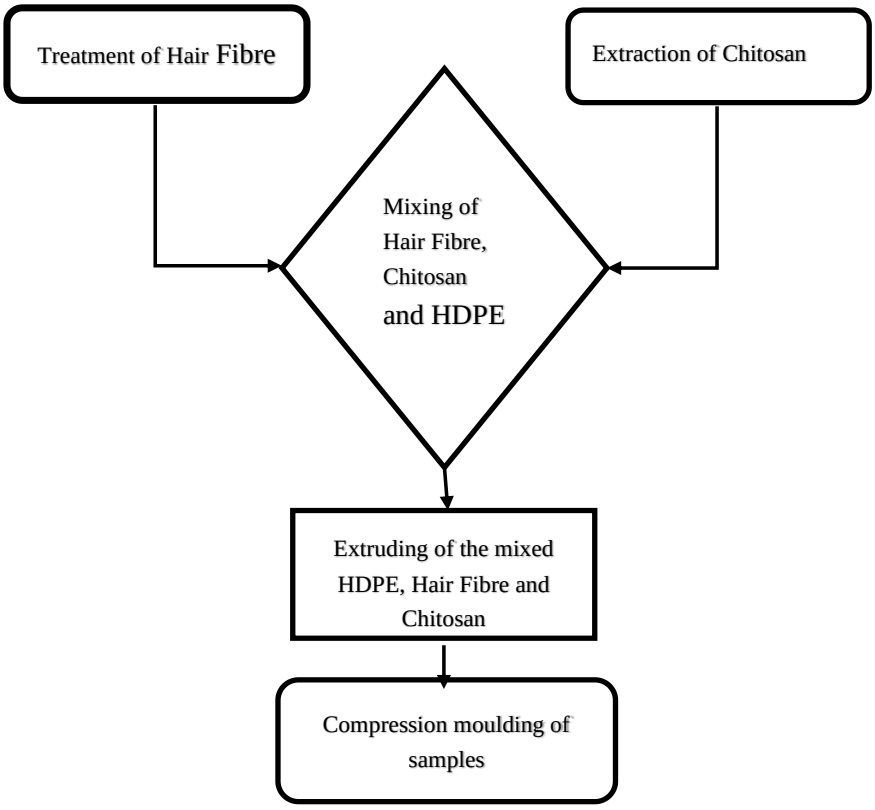

Figure 3: Procedures for Fabrication

MECHANICAL PROPERTIES AND WEAR BEHAVIOUR OF THE COMPOSITES

TENSILE TEST

Using an Instron 5966 tester with a load cell of 10 kN and crosshead speed of 5 mm/minute, tensile tests of the generated composite samples were carried out in accordance with ASTM D638 to ascertain the modulus, ultimate tensile strength, and elongation at break of the samples. The specimens are dog-bone shaped with a gauge length of 25 mm, width of 6.35 mm and a thickness of 3.2 mm. 3 samples were produced for the control sample and 3 samples for each weight percent of the composite developed.

IMPACT TEST

In line with ISO 179, representative samples of the produced composites with dimension 80 mm × 10 mm × 4 mm were subjected to an impact test on a Charpy V-Notch impact testing machine (Instron CEAST 9050). The machine's pendulum, which freely swung across an angle of 180° and fractured the sample, was set up with the notched samples horizontally on it. 3 samples were produced for the control sample and 3 samples for each weight percent of the composite developed.

HARDNESS

The generated composite samples' hardness was assessed using a micro-hardness tester in line with ISO 868. A square specimen was used having a thickness of 6.35mm and a side length of 12.7 mm. A load of 0.5 N was applied at 100 oscillations, the speed of the test was done at 10 Hz at a temperature of 23 ºC and Humidity of 50 %. This device measures the depth of the imprint to determine the resistance to penetration. 3 samples were produced for the control sample and 3 samples for each weight percent of the composite developed.

ABRASIVE WEAR TEST

A wheel or ball was rotated and slid against a fixed sample while being exposed to abrasive particles during an abrasive wear test. The specimen is shaped like a block or a plate with a dimension of 12.7 mm × 6.35 mm according to ASTM G99 standard with Normal Force (10 N), Sliding Speed (0.1 m/s), Temperature (23 ºC), Track Diameter (25-35 mm), Humidity (12-78 %), Pin end Diameter (10 mm), Sliding Distance (1000 m) were all used as the test parameters. Through a loading lever, dead weight regulates contact pressure. A nozzle attached to a hopper above is used to introduce the abrasive particles, such as silica, creating a three-body wear condition. The sample was removed after a predetermined period of running, and wear loss was calculated. Controlled variables included contact load, sliding speed, abrasive particle type, and flow rate. 3 samples were produced for the control samples and 3 sample for each weight percent of the composite developed.

BIOCOMPATIBILITY AND MICROBIAL EVALUATION

MICROBIAL EVALUATION

In order to dislodge the microbial propagules present on the sample into the water, around 2 grams of the samples were crushed and aseptically placed into a bottle containing 9 ml of sterile distill water. The container was then put on a mechanical shaker for about 45 minutes. On nutritional agar plates and potatoes dextrose agar plates, a 1ml amount of each aliquot of the samples was plated. Potato dextrose agar (PDA) plates, utilized for the cultivation of fungi and yeast, were subjected to an incubation period of approximately 48 to 72 hrs at a temperature of 27°C. Concurrently, nutrient agar (NA) plates, designed for bacterial cultivation, were placed within an incubator set at 37°C for a duration of one day. Using laser colony counter, the total number of viable colonies from the plates were counted and recorded accurately per gram of the samples. Subcultures were then performed to produce pure cultures of each isolate. According to the Chauhan and Jindal, (2020) manual for the identification of medical bacteria, individual isolates were identified using a combination of cultural, microscopic, and biochemical assays; isolates of fungus and yeast were identified using Devaraju *et al*. (2021) manual. Coliforms testing was carried out in accordance to Olutiola and Famurewa (1991) using multiple-tube techniques.

BIOCOMPATIBILITY TEST

It was done using Pyar and Peh, (2014) pour plate technique. For culture, the pour plate technique was employed. Using sterile forceps, the material was carefully put into each test tube that contained 9.0 ml of broth containing microorganisms. Each 1ml homogenate was made as a ten-fold serial dilution. After a 24-hour incubation period, precisely 1.0 ml of the

dilution factors 10^{-4} and 10^{-6} were put onto the sterile Petri dishes for culture. After another 24 hrs of bacterial growth incubation at 37°C, the plate was counted. Using a colony counter, colonies were counted in order to determine the overall viable count.

3. RESULTS AND DISCUSSION

FOURIER TRANSFORM INFRARED SPECTROSCOPY (FTIR)

The FTIR analysis of the raw chitosan extracted from crab shell wastes revealed broad bands at 3738, 3000, 2402-2871, 1734 cm^{-1} corresponding to the stretching vibration of N-H and O-H with the extension vibration of N-H and the intermolecular hydrogen bonds of polysaccharide, as well as asymmetric C-H stretching vibration, symmetric C=O stretching vibration, and symmetric N-H stretching vibration. The vibrations caused by the C-N stretching were also the cause of the absorption at 1734 cm^{-1} crab shell waste. The O-H bending vibration in the pyranose ring of the extracted biopolymers was equally linked to the bands at 1344 cm^{-1} (Anand *et al*., 2014). The complex vibrations of the NHCO group, which represent the amide III band, were detected in the raw crab shell waste chitosan at wave number 1244 cm^{-1}. Nevertheless, at 1054 cm^{-1} (crab raw chitosan), a C-O stretching vibration was seen in the alcohol. Additionally, the C-H out-of-plane vibration of the ring of monosaccharides was attributed to the absorption bands and peaks at wavelengths of 840 cm^{-1}, as seen in Figure 4.

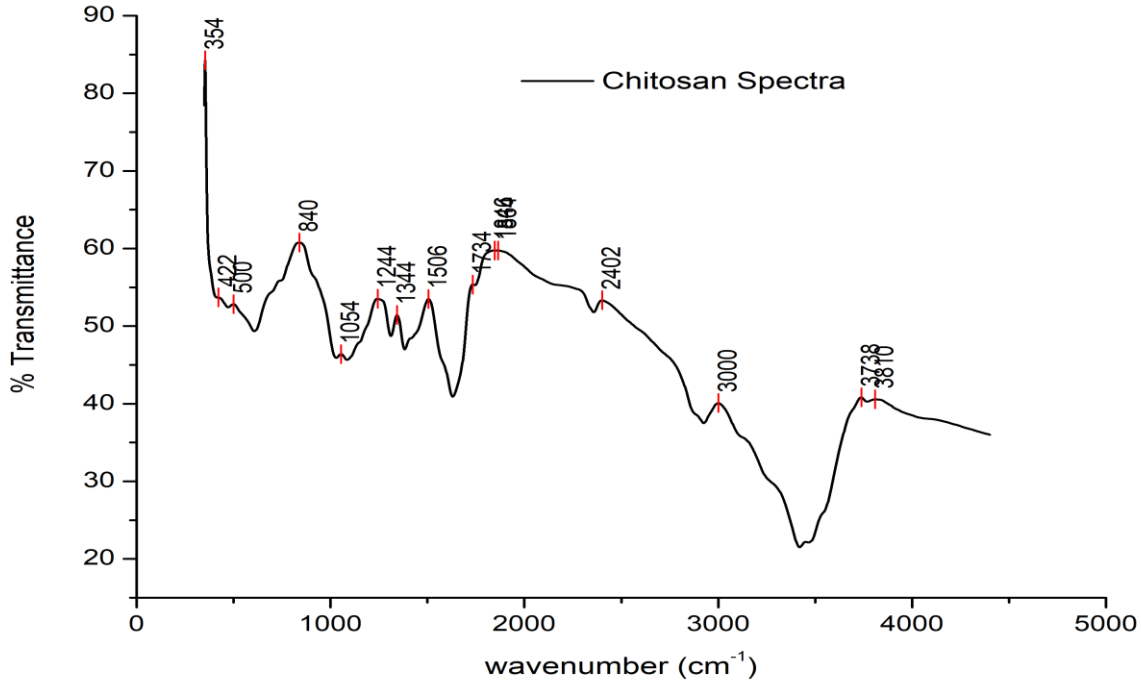

Figure 4. Fourier Transform Infrared Spectroscopic Analysis of Chitosan Particles.

X- RAY DIFFRACTION

The XRD pattern of the chitosan produced by the synthesis of pulverized crab shells was examined. The spectrum was created by plotting intensity (counts) as a function of position (2Θ), and the results are shown in Figure 5. This spectrum shows two distinct peaks at Bragg's angles, 2Θ = 20.0° and 50.0°, as well as numerous minor peaks all around 2Θ that ranges from 40° to 70°. The chitosan's distinctive peaks, which correlate to the crystallographic planes, have centers at 20° and 40° in 2Θ which agrees with Divya *et al*. (2014). Using the XRD data and the Scherrer's and crystallinity equations as presented in equations (1) and (2), the produced chitosan's crystallite size and crystallinity were determined. The crystallinity was 58% and the average crystallite size was 32 nm. Studies have demonstrated that for the same sample, the crystallinity can also vary within a wide range from 57.0 to 93.0% for chitin (Fan *et al*, 2009; Fan *et al*., 2008) and from 40.0 to 80.0% for chitosan (Grząbka-Zasadzinska *et al*., 2017; Pires *et al*., 2014; Yuan *et al*., 2011).

International Journal of Novel Research in Engineering and Science
Vol. 11, Issue 1, pp: (55-71), Month: March 2024 - August 2024, Available at: www.noveltyjournals.com

$$Cystallite\ Size\ (D) = \frac{K\lambda}{\beta Cos\theta} \quad (1)$$

where D is Crystallite size, K is 0.9 (Scherrer's constant), ƛ is 0.15406 nm, β is FWHM (radians), θ is Peak position (radians)

$$Cystallinity = \frac{\text{Area of ctystalline peaks}}{\text{Area of all peaks (cystalline+Amorphous)}} \quad (2)$$

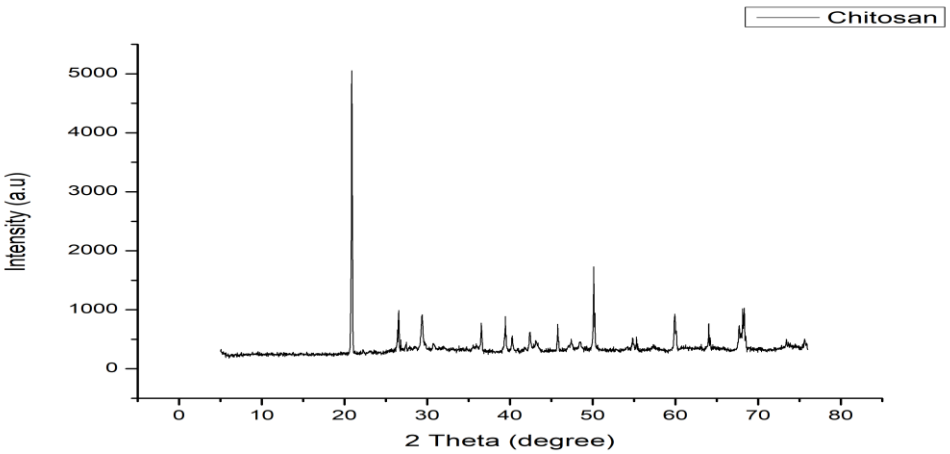

Figure 5. XRD Patterns of Chitosan Particles

Compositional Analysis

The protein-enzymatic systems depend on minerals and trace elements that are vital to the chemical makeup of the hair (Crlab.com). Carbon (45%) is the most abundant chemical element in hair, followed by oxygen (28%) nitrogen (15%) hydrogen (6.7%), and sulfur (5.3%). In addition, a trace mineral analysis revealed the presence of several trace elements, including Ca, K, Na, Mg, Zn, Fe as indicated in Table 2. As stated by Raymond, (2020), bleaching reactions may be the reason for the quick loss of minerals after chemical treatment.

Table 2: Composition of treated and untreated hair fibre

Sample Codes	Metals (mg/100g)					
	Na	K	Ca	Mg	Zn	Fe
Treated hair fibre	1.20	2.50	0.05	0.11	0.22	0.01
Untreated hair fibre	2.22	5.10	0.10	0.15	0.56	0.03

TENSILE PROPERTIES

ULTIMATE TENSILE STRENGTH AND STRAIN TO FRACTURE

The differences in the ultimate tensile strength of the neat HDPE with the developed composites made of chitosan/HF-HDPE were displayed in Figure 6 (a). The sample C with 2.5 weight percent chitosan particles and 2 weight percent HF reinforcement had the highest ultimate tensile strength, measuring 28.43 MPa. As the reinforcement weight fraction increased, the composites exhibited a gradual and linear reduction in their ultimate tensile strength; however, even though the values from samples D through F were higher compared to that of the control sample, the control sample's ultimate tensile strength value was the lowest, measuring 20.01 MPa. Numerous phenomena, including the stress transfer phenomenon, the dislocation interface phenomenon, the Orowan and Hall-Petch phenomenon, can be used to explain the mechanism underlying this behavior. Outstanding load transmission from the matrix to the reinforcement inside the composite resulted from the reinforcement's outstanding particle-fibre interaction. The optimum particle-fibre relationship for efficient stress transmission from the matrix to the reinforcement, highest resistance to dislocation motion, and minimal

or no particle agglomeration was found in Composite C (2.5 wt% chitosan and 2 wt% HF). There was void presence and interfacial debonding at the matrix-reinforcement contact for D-F composites. The investigation of Daramola *et al*. (2019) showed a similar pattern. It is important to highlight that the presence of higher modulus hair fibre integrated into the HDPE matrix, which acted as a barrier to plastic deformation when the composites were subjected to an applied stress, can also be ascribed to the increase in tensile strength.

According to the findings in figure 6 (b), sample F (4wt.% Chitosan+ 5wt.% HF) had the second-highest strain at break after the control sample (A), with a value of 15.25%. The results show that, as sample strength increases, the percentage strain to fracture reduces, indicating that the composite is brittle. Similar trend was observed in the research of Husin *et al*. (2011).

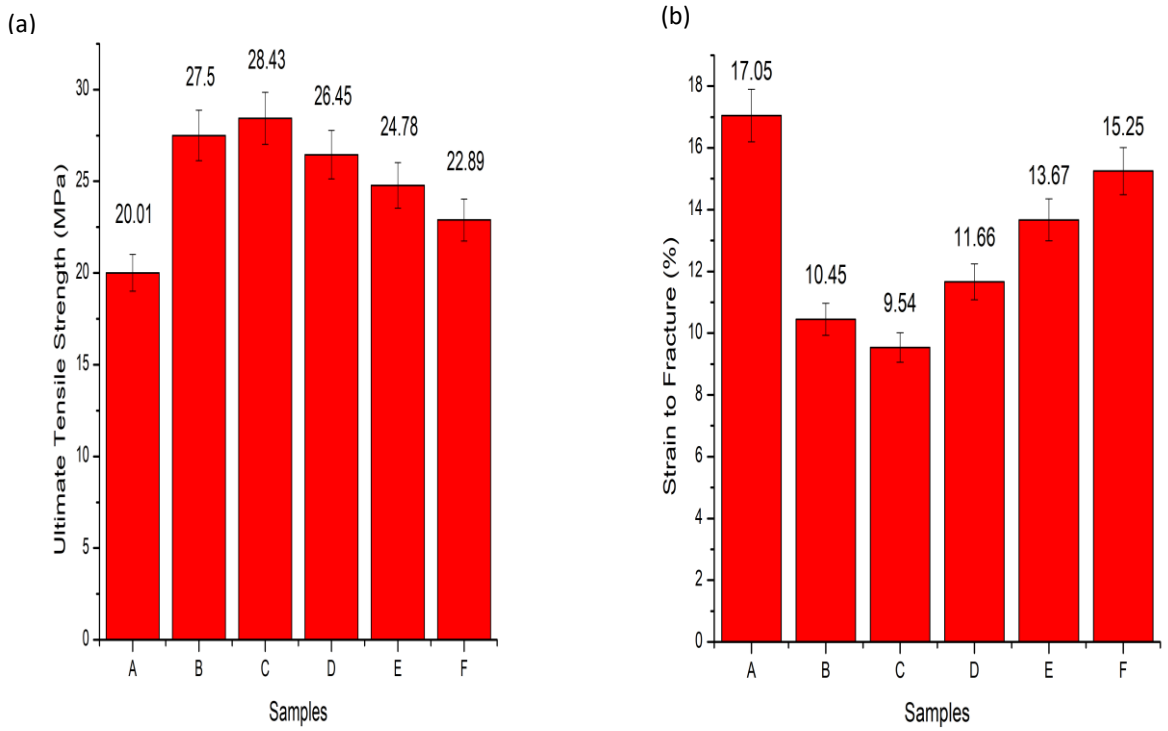

Figure 6 (a) Variations of Ultimate Tensile Strength and (b) Strain to fracture for HDPE Matrix and Chitosan/HF-HDPE Composites.

YOUNG'S MODULUS

The ratio of the stress along an axis over the strain along the same axis in which the Hook's law holds is known as the Young's modulus, and it represents the stiffness of a material. Nearly all of the samples exhibited noteworthy results, according to Figure 7. The performance of the composites was excellent. It was found that increasing the composite's reinforcement content increased the tensile modulus of samples B and C, resulting in values of 375.45 MPa and 400.36 MPa, respectively. These findings are attributed to the incorporation of chitosan/HF into the polymer matrix, leading to a synergistic enhancement of the composites' tensile modulus. Nonetheless, samples D through F exhibited a reduction in their Young's modulus properties. This decrease is attributed to the presence of voids within the matrix, insufficient particle-fibre interaction, and inadequate interfacial adhesion between the matrix and the reinforcement, resulting in ineffective stress transmission at the interface. A study by Daramola *et al*. (2021) demonstrated a comparable trend.

Novelty Journals

ISSN 2394-7349

International Journal of Novel Research in Engineering and Science
Vol. 11, Issue 1, pp: (55-71), Month: March 2024 - August 2024, Available at: www.noveltyjournals.com

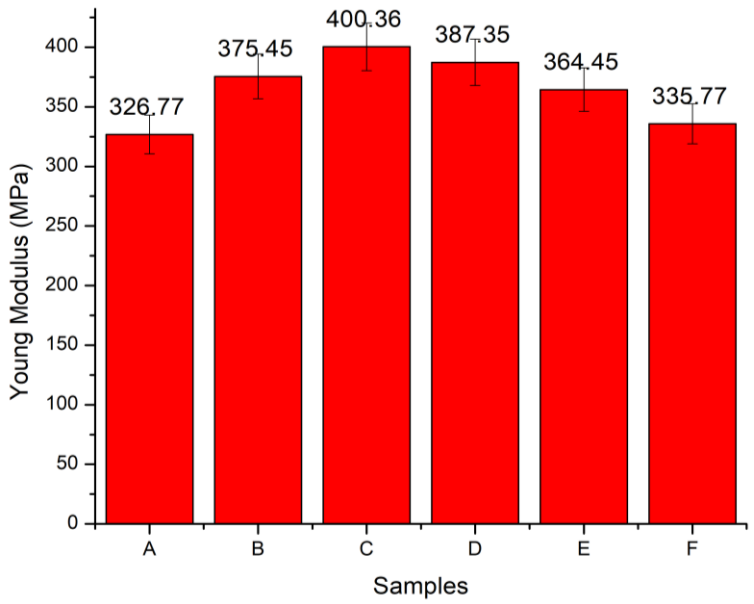

Figure 7: Variations of Young's Modulus for HDPE Matrix and Chitosan/HF-HDPE Composites.

HARDNESS

The hardness values of the control sample as well as the produced composites are clearly displayed in Figure 8. It is obvious from the chart that the developed HDPE composites have greater hardness values than the unreinforced sample. The hardness value of the produced composites rises linearly up to 3 weight percent chitosan and 3 weight percent HF (sample D), which has a hardness value of 51.52 HS, only a little higher than sample C's hardness value of 50.23 HS, before also declining linearly. This result aligns with the findings of Ilyas *et al*. (2022).

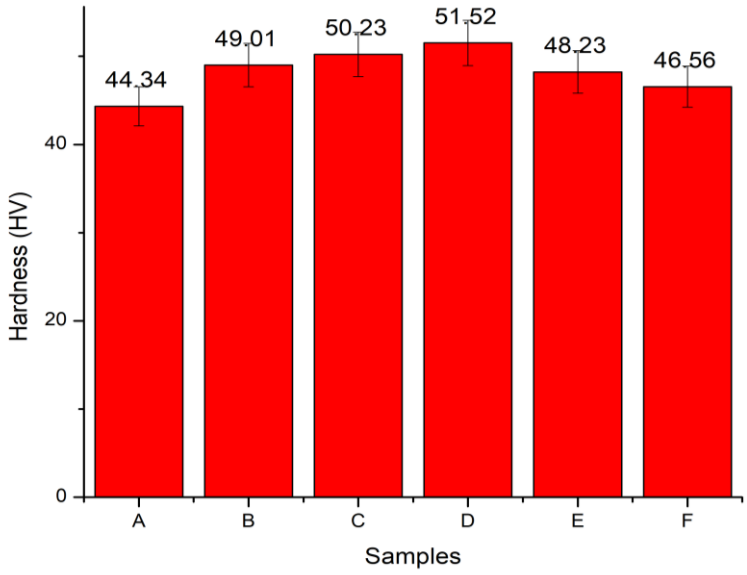

Figure 8. Variations of Hardness properties for HDPE Matrix and Chitosan/HF-HDPE Composites.

IMPACT STRENGTH

The composite samples exhibited a consistent rise in impact strength, with the D sample having the greatest impact value at 32.67 KJ/m^2, according to the plot shown in Figure 9. Researcher Leong *et al*. (2003) found that fillers are mostly responsible for enhancing the impact characteristics of biopolymer composites. The impact energy does, however, diminish

when the chitosan/HF filler percentage is raised to 3.5/4wt% and 4/5wt% compositions, respectively. This is because there is inadequate interfacial adhesion between the matrix and the fillers, which creates sites for fracture initiations and causes the composite's impact strength to drop sharply. This result is consistent with the study conducted by Giita *et al*. (2012). With an impact energy value of 21.85 KJ/m^2, the control sample produced the least favorable results. This is because there were no reinforcing materials present.

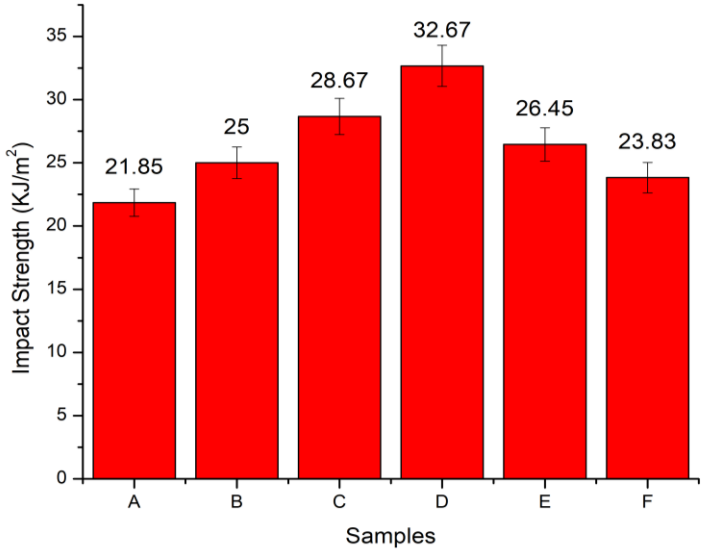

Fig 9: Variations of Impact strength for HDPE Matrix and Chitosan/HF-HDPE Composites.

WEAR/ABRASION PROPERTY

The purpose of the wear test was to assess the composite materials' wear characteristics and decide whether they were appropriate for a given wear application. With the exception of sample B, which has a wear rate value of 0.04 mm^3/Nm, the composites produced demonstrated superior wear resistance than the control sample (HDPE) according to the results in Figure 10. Additionally, sample D with 3 weight percent chitosan and 3 weight percent HF reinforcement had the optimum wear behavior. This is because the reinforcement and HDPE matrix were well bonded, which also helped to improve the shearing mechanism and create the stress distribution over the interface. This finding disagrees with the findings of Constantin and Iuliana, (2014).

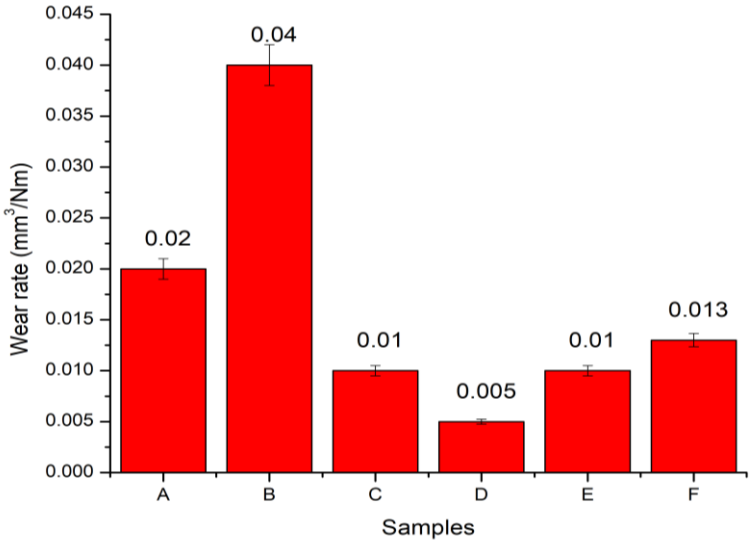

Figure 10: Variations of wear loss for HDPE Matrix and Chitosan/HF-HDPE Composites.

Novelty Journals

ISSN 2394-7349

International Journal of Novel Research in Engineering and Science
Vol. 11, Issue 1, pp: (55-71), Month: March 2024 - August 2024, Available at: www.noveltyjournals.com

3.8 SCANNING ELECTRON MICROSCOPY

The morphology of the fractured HDPE surface (control sample) and Chitosan/HF composites is shown in Figure 9. The clean HDPE matrix's SEM picture is displayed in Figure 11 (a). This is a sign of a ductile mode of fracture due to the roughness of the fracture surfaces, which is consistent with the findings of the mechanical tests done on the composites. Chitosan/HF reinforcement filling the ductile HDPE matrix is seen in Figure 11 (b). The reinforcements were not properly distributed throughout the matrix, making it difficult to effectively block dislocation motion and withstand applied forces even though there is no void emergence. The shattered surface with uniform distribution and improved orientation of chitosan particles and HF was shown in Figure 11 (c) and (d). The improved results of ultimate tensile strength, modulus of elasticity, hardness, and impact strength as shown in Figures. 6, 7, 8, and 9 respectively, indicate that this effect increases the interaction at the interface between fillers and matrix, which helps to dissipate stresses and increase mechanical properties of the composite. The voids in the chitosan/HF-HDPE composite increased as a result of an increase of reinforcing materials, as seen in Figures 11 (e) and (f). The fracture mode was rather brittle. This is due to the fact that the voids function as stress raisers, causing the material to fail or fracture under lower applied stress.

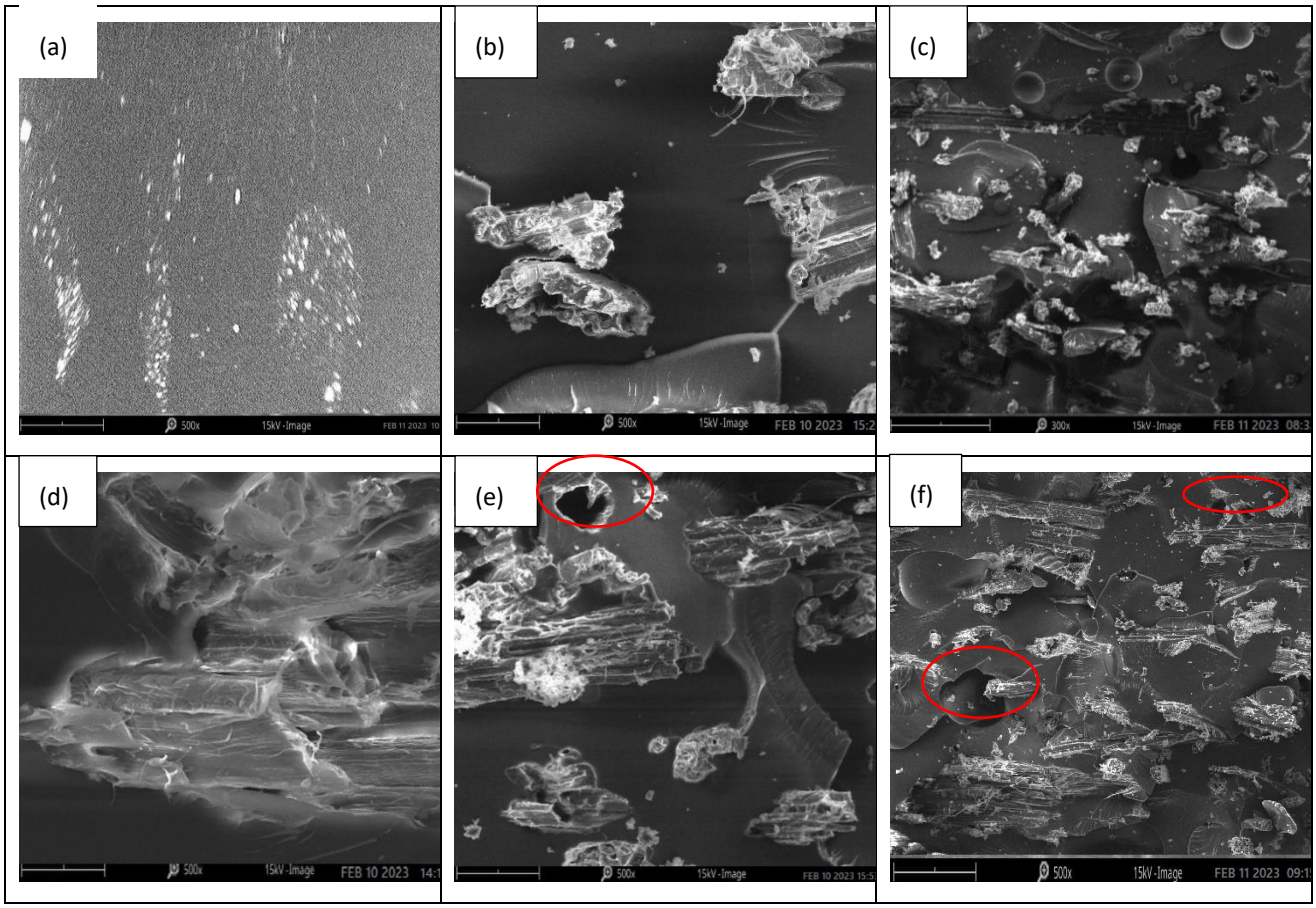

Figure 11. SEM micrograph of (a) Control sample (b) 2wt.% chitosan + 1wt HF (c) 2.5wt.% chitosan + 2wt HF (d) 3wt.% chitosan + 3wt HF (e) 3.5wt.% chitosan + 4wt HF (f) 4wt.% chitosan + 5wt HF.

MICROBIAL EVALUATION

As it can be seen in Figure 12, it was found that all of the samples (unsterilized) produced a higher microbial population. The microbes associated with the samples are probably contaminants from the environment picked up during handling, as well as from packing materials and non-sterilized materials used in the production of the samples. The data clearly show that yeast colony forming units and bacteria load both significantly increase with an increase in reinforcement weight percent. Additionally, all of the unsterilized samples (A-F) revealed no coliform count and only sample E revealed the existence of a fungus colony with 2 cfu/g. The developed composite is most suitable for the intended purpose when it is

sterilized because when the samples were sterilized at 105°C for 15 minutes, no microbial growth was observed. The samples were stable and able to withstand the heat of sterilization (i.e., the materials are relatively thermo stable). This finding aligns with the research conducted by Balouiri *et al*. (2016).

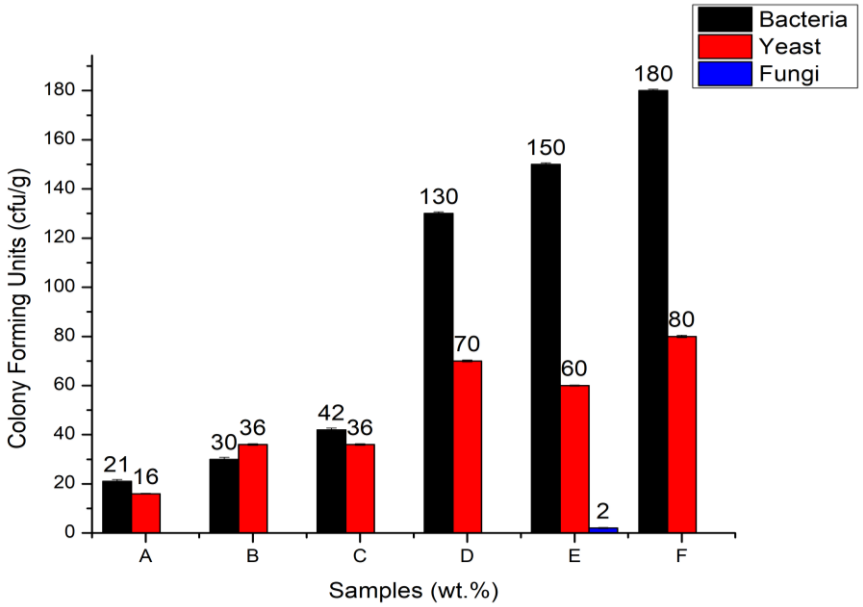

Figure 12: Microbial Population Plots for HDPE Matrix and Chitosan/HF-HDPE Composites for Bacteria Load, Fungi Colonies and Yeast.

BIOCOMPATIBILITY

The average Total Plate Count for all samples is shown in Figure 13 as CFU/ml. It shown that the sample F has the lowest capacity to sustain bacterial growth whereas the unreinforced sample A has the maximum potential. However, Sample D appears to exhibit a typical affinity for the bacterial community. This indicates that sample F is the best for biomedical applications since it has a total average colony count of 122 CFU/ml, which is lower than all other samples with greater total average colony counts. As a result, it is clear that the unreinforced sample has a high affinity for microbial growth and is therefore more likely to cause infections, whereas sample F exhibits greater resistance to harmful microbial growth and is thus less likely to result in diseases like osteomyelitis, a bacterial or fungal infection of the bone. This observation is in line with the findings reported by Poliana *et al*. (2019).

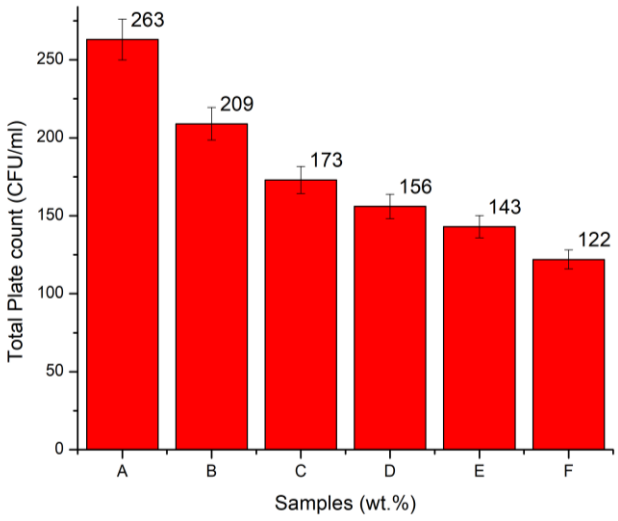

Figure 13: Biocompatibility of HDPE Matrix and Chitosan/HF-HDPE Composites in CFU/ml

4. CONCLUSIONS

The following conclusions are drawn from this study's findings about the development of chitosan-human hair fibre reinforced high density polyethylene (HDPE) biocomposite for biomedical applications:

i. By successfully transferring stress, the chitosan particle and human hair fibre performed well as reinforcement, outperforming the plain HDPE polymer matrix in terms of the composites' mechanical characteristics.

ii. Compared to the unreinforced material, the produced composites demonstrated superior improvement in mechanical and wear characteristics. The composites' best tensile strength and tensile modulus were found at 2.5 weight percent chitosan + 2 weight percent HF (sample C) reinforcement, with values of 28.43 MPa and 400.36 MPa, respectively. The best hardness was found at 3 weight percent chitosan + 3 weight percent HF (sample D), with hardness value of 51.52 HV. The composites' impact strength increased steadily, with the D sample having the maximum impact value at 32.67 KJ/m^2. Additionally, it was noted from the findings that as composite strength increases, % elongation decreases. According to the wear test, sample D with 3 weight percent chitosan and 3 weight percent HF reinforcement exhibited the best wear behavior.

iii. The produced composite had good biomedical qualities. The produced composite demonstrates that sample F, which contains 4 weight percent chitosan and 5 weight percent HF, has the lowest capacity to promote bacterial growth whereas control sample has the maximum ability. This indicates that the sample is more likely to support cell viability, and the microbiological analysis revealed that unsterilized samples acquired a significant number of microorganisms (fungi, bacteria, yeast, and coliform) as a result of material handling during manufacturing or just before the test was conducted. The sterilized samples exhibited no evidence of microorganisms and were found to be thermostable.

iv. In order to achieve sustainable development by reusing trash to make value-added products for enhancing the quality of human life, a new method to the production of biomaterials from the combination of animal waste and human hair has been established.

AUTHOR'S CONTRIBUTIONS:

DOO, ATA, ABO, OA, AAS, OOO wrote the main manuscript text and DOO, ATA, AAA, ABO, OA, AAS, OOO prepared figures. All authors reviewed the manuscript

ACKNOWLEDGEMENT:

The authors acknowledged the financial support received from Tertiary Education Trust Fund (TETFund) through Institution Based Research (IBR) intervention, with reference number, TETF/DR&DICE/UNI/AKURE/IBR/2022/VOL.II

Consent for publication: All authors agreed upon the current version of submission for publication.

Data availability: The datasets used and analyzed during the current study available from the corresponding author on reasonable request.

Ethics approval: Not applicable.

Conflict of Interests: The authors declare that they have no known competing financial interests or personal relationships that could have influenced the work reported in this paper.

REFERENCES

[1] Anand, M., Kalaiv, R., Maruthupandy, M., Kumaraguru, A.K. and Suresh. S., Extraction and characterization of chitosan from marine crab and squilla collected from the Gulf of Mannar Region, South India, *Journal of Chitin and Chitosan Sciences*, No.**2**, pp. 280 – 287, 2014

[2] Babu R. J., Mathew S., Jacob S.R., Abraham J., and George S.C. (2021): Human hair reinforced natural rubber composite: effect of hair loading on mechanical, structural, morphological and thermal behavior, *Journal of Rubber Research*, No. 24, pp.347–354, 2021

[3] Balaji, S., Kumar, R., Sripriya, R., Rao, U., Mandal, A., Kakkar, P., Reddy, P.N. and Sehgal, P.K., Characterization of Keratin–Collagen 3D Scaffold for Biomedical Applications. *Polymers for Advanced Technologies*, **23**(3): 500-507, 2012

[4] Balouiri, M., Sadiki, M. and Ibnsouda, S. K., Methods for in vitro evaluating antimicrobial activity: A review. *Journal of Pharmaceutical Analysis*, **No. 6**, Issue 2, pp. 71–79, 2016.

[5] Butt W. A., Mir B. A. and Jha J. N., "Strength behavior of clayey soil reinforced with human hair as a natural fibre," *Geotech. Geol. Eng*., No. **34**, pp.411-417, 2016

[6] Choudhry S., and Pandey B.,"Mechanical behaviour of polypropylene and human hair fibres and polypropylene reinforced polymeric composites," *Int. J. Mech. Ind. Eng*., Issue **2**, No.1, pp.118-121, 2012

[7] Constantin E. T and Iuliana S., PLA/chitosan/keratin composites for biomedical applications. *Materials Science and Engineering C*, No, 40. pp. 242-247, 2014

[8] Croisier, F. and Jérôme, C., Chitosan-Based Biomaterials for Tissue Engineering. *European Polymer Journal*, Issue 4**9,** No. 4, pp. 780-792, 2013.

[9] Daramola O. O, Taiwo, A. S. Oladele, I. O. Olajide, J. L. Adeleke, S.A. Adewuyi B.O. and Sadiku E. R., Mechanical properties of high - density polyethylene matrix composites reinforced with chitosan particles, *Materials Today: Proceedings*, No. **38**, pp. 682-687, 2021

[10] Daramola, O. O., Olajide, J. L., Agwuncha, S. C., Mochane, M. J. and Sadiku, E. R., Nanostructured Green Biopolymer Composites for Orthopedic Application, A Book Chapter in *Green Biopolymers and Their Nanocomposites, Materials Horizons: From Nature to Nanomaterials, 2019.*

[11] Devaraju, R., Subbanna, S. and Narasimha, G., Identification of Individual Isolates using Cultural, Microscopic, and Biochemical Tests. *Journal of Microbiological Methods*, No. **98**, pp. 123-135, 2021

[12] Divya, K., Sharrel, R. and Jisha, S., A Simples and effective Method for extraction of High Purity Chitosan from shrimp shell waste, International Conference in applied Science and Environmental Engineering, pp. 2-3, 2014.

[13] Fan, Y., Saito, T. and Isogai, A., Chitin nanocrystals prepared by TEMPO-mediated oxidation of α-chitin. *Biomacromolecules*, Issue **9**, No. 1, pp. 192–198, 2008

[14] Fan, Y., Saito, T. and Isogai, A., TEMPO-mediated oxidation of β-chitin to prepare individual nanofibrils. *Carbohydrate Polymers*, **77**(4): 832–838, 2009

[15] Fatnah N., Dewiantika A. and Mutiara D. C., Synthesis of Chitosan from Crab's Shell Waste (Portunus pelagicus) in Mertasinga-Cirebon, *Advances in Social Science, Education and Humanities Research*, 422, 2019

[16] Fukunishi, T., Best, C. A., Sugiura, T., Shoji, T., Yi, T., Udelsman, B., Ohst, D., Ong, C. S., Zhang, H., Shinoka, T., Breuer, C. K., Johnson, J. and Hibino, N., Tissue-Engineered Small Diameter Arterial Vascular Grafts from Cell-Free Nanofibre PCL/Chitosan Scaffolds in a Sheep Model. *PloS one*, No. ***11,*** No. 7, e0158555, 2016

[17] Giita V.S. Silverajah, A.I. Nur, Z. Norhazlin, Wan, M. and Hazimah A.H. (2012): Mechanical, thermal and morphological properties of poly (lactic acid)/epoxidized palm olein blend, *Open Access Molecules*, No. **17,** 117, pp. 29 –11747, 2012

[18] Grząbka-Zasadzinska, ´ A., Amietszajew, T. and Borysiak, S. (2017): Thermal and mechanical properties of chitosan nanocomposites with cellulose modified in ionic liquids. *Journal of Thermal Analysis and Calorimetry*, Issue **130,** No.1, 143–154.

[19] Hiwarkar V. G., Lanjewar, P. S. Bonode, A. D. and Somnathe S. V. "Hair fibre reinforced concrete," *Int. J. Res. Sci. Eng*., No. **3**: pp. 1-12, 2017

[20] Husin M. R., Mat U. W., Mohammed R. K. and Wan A. A. (2011): Effect of Hydroxyapatite Reinforced High Density Polyethylene Composites on Mechanical and Bioactivity Properties, *Key Engineering Materials*, Issue 471, p. 47, 303-308

[21] Ilyas, R. A.; Aisyah, H. A., Nordin, A. H., Ngadi, N.; Zuhri, M. Y. M., Asyraf, M. R. M., Sapuan, S. M., Zainudin, E. S., Sharma, S. and Abral, H., Natural-Fibre Reinforced Chitosan, Chitosan Blends and Their Nanocomposites for Various Advanced Applications, *Polymers*, No. 14, p.874, 2022

[22] Jain D. and Kothari A. "Hair fibre reinforced concrete," *Res. J. Recent. Sci*., No. **1**, pp.128-133, 2012

[23] Jayathilakan, K., Sultana, K., Radhakrishna, K. and Bawa, A. S. Utilization of Byproducts and Waste Materials from Meat, Poultry and Fish Processing Industries: A Review. *Journal of Food Science and Technology*, Issue 49**,** No. 3, pp. 278-293, 2012

[24] Kumar, G., De, S., Franco, A., Balu, A.M. and Luque, R., (2015): Sustainable Biomaterials: Current Trends, Challenges and Applications. *Molecules*, Issue 21, No. 1, p. 48.

[25] Lam M. T. and Wu J. C., Biomaterial applications in cardiovascular tissue repair and regeneration, *Expert Rev. Cardiovasc. Ther*. No. 10, pp. 1039–1049, 2012

[26] Lee, J.B., Park, H.N., Ko, W.K., Bae, M.S., Heo, D.N., Yang, D.H. and Kwon, I.K., Poly (L-lactic acid)/Hydroxyapatite Nanocylinders as Nanofibrous Structure for Bone Tissue Engineering Scaffolds. *Journal of Biomedical Nanotechnology*, Issue 9**,** No.3, pp. 424-429, 2013

[27] Leong Y. W., Abu, M. B. Mohd, I. and Ariffin A. (2003): Characterization of talc/calciumcarbonate filled polypropylene hybrid composites weathered in a natural environment, *Polym. Degrad. Stab.* No. **83**, pp. 411 –422, 2003

[28] Manivasagam, G., Dhinasekaran, D. and Rajamanickam, A., Biomedical Implants: Corrosion and its Prevention-A Review. *Recent Patents on Corrosion Science*, No. **2**: pp. 40-54, 2010

[29] Nanda B. P., and Alok Satapathy, "Processing and characterization of epoxy composites reinforced with short human hair," IOP Conf. Series: *Mater. Sci. Eng*.,No. 178, pp. 1-6, 2017

[30] Olutiola P. O. and Famurewa, H. G., An introduction to general microbiology. A practical approach. No. **3**, pp. 101-11, 1991

[31] Paxton N. C., Allenby M.C., Lewis, P.M. and Woodruff M.A., Biomedical applications of polyethylene, *Eur. Polym. J.*, pp. 412–428, 2019

[32] Pires C. T. G. V. M. T., Vilela, J. A. P. and Airoldi, C., The effect of chitin alkaline deacetylation at different condition on particle properties. *Procedia Chemistry*, No. **9**: 220–225, 2014

[33] Poliana S. L., Rossanna T., Renate M. W., Luis R., Miguel A. L., Marcus V.L. F. and Suedina M.L.S., HDPE/Chitosan composites modified with PE-g-MA.Thermal, Morphological and Antibacterial Analysis, *Polymer (Basel). Issue* **10**, No.11, 1559, 2019

[34] Prashant S. and Shishir S., Effect of alkali treatment on hair fibre as reinforcement of HDPE composites: mechanical properties and water absorption behavior, *Sci Eng Compos Mater*; Issue **25,** 3, pp. 571-578, 2018

[35] Puppi D., F. Chiellini, A. M. and Piras, C.E., Polymeric materials for bone and cartilage repair, *prog.Polym. Sci.* No. **35**: pp, 403–440, 2010

[36] Pyar H and Peh K., Enteric coating of granules containing the probiotic *Lactobacillus acidophilus, Acta Pharm*. No. **64**:, pp.247-256, 2014

[37] Raymond F. L, Effect of Washing on trace element content of human hair, Journal of Orthomolecular Medicine, No. **1**, p. 2, pp. 120-125, 2020

[38] Saini, M., Singh, Y., Arora, P., Arora, V. and Jain, K., (2015): Implant Biomaterials: A Comprehensive Review. *World Journal of Clinical Cases:WJCC*, Issue **3**, No. 1, p. 52.

[39] Schmutz, P., Quach-Vu, N.C. and Gerber, I., Metallic Medical Implants: Electrochemical Characterization of Corrosion Processes. *The Electrochemical Society Interface*, Issue **17**, No. 2, p. 35., 2008

[40] Scholz, M. S., Blanchfield, J. P., Bloom, L. D., Coburn, B. H., Elkington, M., Fuller, J. D., Gilbert, M. E., Muflahi, S. A., Pernice, M. F., Rae, S. I. and Trevarthen, J. A., (2011): The Use of Composite Materials in Modern Orthopedic Medicine and Prosthetic Devices: A Review. *Composites Science and Technology*, Issue **71**, No. 16, pp. 1791-1803, 2011

[41] Tran C. D. and Mututuvari, T. M., Cellulose, Chitosan and Keratin Composite Materials: Facile and Recyclable Synthesis, Conformation and Properties. *ACS Sustainable Chemistry & Engineering*, Issue **4,** p. 3, pp. 1850-1861, 2016

[42] Vengatesan K. J., Prasanth, T. Swagath K. S., Suresh, K. and Chokkalingam P., "Study on mechanical properties and structural analysis of human hair fibre reinforced epoxy polymer," *Int. J. Adv. Res. Basic Eng. Sci. Technol.*, No. **3**, pp.754-759, 2017

[43] Wang M., Developing bioactive composite materials for tissue replacement, *Biomaterial*., No. **24**, pp. 213–215, 2003

[44] Yuan Y., Chesnutt, B. M., Haggard, W. O. and Bumgardner, J. D. (2011): Deacetylation of chitosan: Material characterization and in vitro evaluation via albumin adsorption and pre-osteoblastic cell cultures. Materials, **Issue 4**, No. 8, pp. 1399–1416, 2011

[45] Zhao, Z. Sun, J. Wang, Y. Xu, L. Li, Y. and Ge. Electrochemical Properties of a Highly Biocompatible Chitosan Polymer Actuator Based on a Different Nanocarbon/Ionic Liquid Electrode.*Polym. Compos,* Issue **38, No.** 11, p. 2395, 2017

[46] Zirak H. K., Ghaee, A. Mashak, A. and Mohammadnejad J. (2017): Preparation of chitosan–silica/PCL composite membrane as wound dressing with enhanced cell attachment. *Polym. Adv. Technol*, Issue 28, No. 11, p. 1396, 2017